

The Synthesis and Characterization of Low-cost Mesoporous Silica SiO₂ from Local Pumice Rock

Regular Paper

Asmaa Mourhly¹, Mariam Khachani¹, Adnane El Hamidi¹, Mohammed Kacimi¹,
Mohammed Halim¹ and Said Arsalane^{1*}

¹ Laboratory of Materials, Catalysis and Environment (CNRST-URAC 26), University of Mohammed V, Faculty of Sciences, Rabat, Morocco
*Corresponding author(s) E-mail: Pr.saidarsalane@gmail.com

Received 18 August 2015; Accepted 23 November 2015

DOI: 10.5772/62033

© 2015 Author(s). Licensee InTech. This is an open access article distributed under the terms of the Creative Commons Attribution License (<http://creativecommons.org/licenses/by/3.0>), which permits unrestricted use, distribution, and reproduction in any medium, provided the original work is properly cited.

Abstract

Pumice is a porous volcanic rock containing a significant proportion of silica and alumina, and which has a low iron content. This natural, silica-rich material attracts wide attention because of its applications in adsorption processes, heterogeneous catalysis and nanotechnology. In this contribution, the white amorphous silica nanoparticles were extracted using an optimized alkaline treatment and an acid-precipitation process using grey pumice powder. The isolated amorphous silica SiO₂ was characterized via X-Ray Diffraction (XRD), Fourier Transform Infrared Spectroscopy (FTIR), Transmission Electronic Microscopy (TEM-EDS), N₂ adsorption/desorption measurements and simultaneous Thermal Gravimetry/Differential Thermal Analysis (TG/DTA). The obtained results indicated that the nanosilica powder was successfully prepared via the acid-base route with a predominantly amorphous mesoporous structure having a high surface area (422m²/g). The TEM images exhibited relatively homogeneous dispersed nanosilica particles with small sizes about 5–15 nm, in accordance with XRD data. Thermal analysis of the silica powder under air atmosphere showed total mass losses of 6.5%, with endothermic effects corresponding to the

removal of water molecules and the OH of silanol groups contained in the material. The investigations performed in this work have indicated that there is great scope for pumice exploitation as a raw material in the production of amorphous silica nanopowder on large scale.

Keywords Pumice rock, Amorphous silica, Nanoparticles, Surface area

1. Introduction

Pumice is a cheap and abundant vesicular rock of volcanic origin, formed by the combination of SiO₂ and Al₂O₃ at variable proportions. It can be found in many regions of the world and has been used as a raw material in several fields, such as an adsorbent in environmental applications [1], an additive in the cement industry [2], a low-cost reinforced filler and filter materials [3]. The natural variability of pumice's composition allows for a wide range of physical and chemical properties, which provides the opportunity for upgrading this mineral resource. It can be utilized to obtain various synthetic zeolites with open framework structures, using hydrothermal and sol-gel processes [4–6].

Recently, the production of silica from cheap raw materials has attracted much attention because it is more economical than conventional methods, which are based on the synthesis of pure silica from tetraethyl-orthosilicate (TEOS) using the sol-gel process [7, 8] or from quartz sand by alkaline-melting at high temperature [9]. Nevertheless, the commercial methods remain very expensive and energy intensive.

Natural perlite is one of the cost-effective raw materials that have been used for extracting non-crystalline silica with high reactivity. Two distinct forms have been isolated, depending on the process conditions. The first form is aggregated particles of colloidal dimensions and the second is fine-powder amorphous silica with a large surface area, obtained by coagulation of particles from an aqueous solution [10]. Both materials have many potential applications, such as catalyst supports [11, 12], in pharmaceuticals [13], in vegetable-oil refining [14] and in thin films or coatings for electronic and optical materials [15, 16].

Another efficient way to produce amorphous silica based on the low-temperature alkali extraction method has been used on agricultural and industrial wastes such as fly ash [17], rice-husk ash [18, 19] and biomass [20]. The advantage of the method is to reduce solid wastes generated by various industries by transforming them into useful products. In addition, the alkali treatment gives rise to controlled particles of nanosilica with adjustable porosity and a large surface area, which are valued in heterogeneous catalysis and actual technological uses.

The present work is a contribution to the production of economical amorphous silica, which will be used in the second part of this research as a support catalyst for the dry reforming of methane at an ambient pressure for hydrogen production. This paper deals with the extraction method of amorphous silica material from local pumice rock, which is abundantly available in many parts of Morocco, by using acid-base leaching. This easy and effective procedure leads to the production of nanosilica materials with special properties. In order to identify the main physicochemical characteristics of extracted silica, it was examined by X-ray diffraction, FTIR spectroscopy and thermal analysis. Identification of the particles' texture and morphology was performed using MET-EDS microscopy, and the surface area was measured via the BET method.

2. Experimental section

2.1 Materials

The material used for the synthesis of porous silica is a natural pumice rock obtained from the Middle Atlas Mountains region in the south of Morocco. The light grey colour of this raw material is due to the presence of iron species. All chemical reagents with the highest available purity, including NaOH, H₂SO₄ and HCl, were supplied by Merck and used as received without further purification.

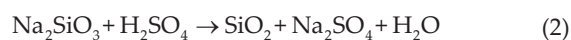
2.2 Preparation of pumice

First, natural pumice rock was washed several times with distilled water before use, in order to remove any impurities, dried overnight at 90°C to evaporate the moisture and then crushed in a mortar. The crushed pumice was ground well and passed through a 180 µm sieve for chemical and mineralogical analyses, then washed and thermally activated at 500°C for three hours.

2.3 Nanosilica extraction

A simple and effective, optimized chemical process is described for extracting silica from pumice powder. Mixed with 150 ml of NaOH (3M) were 2.5 g of pumice, in a 250 ml neck flask equipped with a reflux condenser. The mixture was maintained at a constant heat (100°C) and stirred at 300 rpm for 24 hours to dissolve the silica and produce sodium silicate. The resulting slurry was then filtered through an ashless filter (Whatman N° 41) and washed with the minimum necessary amount of boiled distilled water. Silica starts to precipitate when the pH of the mixture falls to less than 10; thus, the acidic conditions were maintained until the complete precipitation of silica was achieved. An acidification and neutralization of the transparent filtrate solution was performed to form a silica gel; therefore, the solution was titrated with H₂SO₄ (5M) to pH 7 while being stirred vigorously. The soft, white aqua gel that formed was allowed to stand at room temperature for 24 hours, before being filtered and washed with distilled water to remove the sulphate salt. The solid residue was dried at 80°C for 24 hours. To purify the silica from the soluble minerals Al, Ca, Fe and Mg, the powder was refluxed with a solution of hydrochloric acid HCl (1M) at 110°C for three hours. The suspension was filtered and washed with copious amount of distilled water, and oven-dried at 110°C overnight. Calcination at 800 °C for two hours using a muffle furnace was the last step of the process, in which a fine silica powder was obtained with an excellent mass yield of 94%. The colour of pumice powder after treatment was changed from light grey to a white colour.

The chemical equations involved in the process of synthesizing silica powder are:



3. Characterization of samples

To investigate and check the characteristics of the pumice powder and extracted silica, X-Ray Diffraction (XRD) data were collected at room temperature using an X-ray diffractometer (Siemens D 500) with copper anticathode radiation ($\lambda_{\text{CuK}\alpha} = 1.541838 \text{ \AA}$) at 2θ from 10 to 90°. Fourier Transform

Infrared (FTIR) spectra were obtained on a Vertex 70 spectrometer equipped with a Digitec detector, via the conventional KBr pellet method. The samples were scanned in transmission mode with 4 cm^{-1} resolution, at the range of 4000 to 400 cm^{-1} . Transmission Electronic Microscopy (TEM-EDS) micrographs were obtained with a Tecnai G2 (produced by the produce by the FEI company) operating at 120 kV with 0.35 nm resolution, and which was equipped with an EDS micro-analyser. Before analysis, the sample was dispersed in ethanol, then deposited onto a copper grid and dehydrated under a vacuum. X-Ray Fluorescence Spectroscopy (XRF, Panalytical Epsilon 5) was applied to determine the chemical bulk composition of the raw materials. The Brunauer-Emmett-Teller (BET) surface area, pore size and pore volume of materials were analysed using a nitrogen adsorption-desorption instrument (the Micromeritics Tristar II 3020 porosimeter). Samples were measured after degassing at $100\text{ }^\circ\text{C}$ for three hours. The porosity and pore-size distribution was calculated using the Barrett-Joyner-Halenda (BJH) method. The simultaneous thermogravimetry and differential thermal analysis (TG/DTA) analyses were carried out using a Labsys™Evo (1F) Setaram apparatus. An initial mass of the sample, about $10 \pm 0.4\text{ mg}$, was placed in an alumina crucible. The measurements were conducted under non-isothermal conditions in air atmosphere (60 ml/min^{-1}) from an ambient temperature up to $900\text{ }^\circ\text{C}$, using a heating rate of $10\text{ }^\circ\text{C/min}^{-1}$.

4. Results and discussion

4.1 Chemical analysis

The chemical and phase compositions of the raw pumice powder are given in Table 1. As result of chemical analysis, the main components were discovered to be SiO_2 and Al_2O_3 with the average amounts of 48% and 14.9% , respectively. Moreover, an appreciable iron oxide content (6.71%) is observed, which is compatible with the grey colour of the raw pumice [21]. Other oxides have also been detected, such as MgO , Na_2O , CaO and K_2O .

Oxide	SiO_2	Al_2O_3	MgO	Na_2O	CaO	Fe_2O_3	K_2O	Others	L.O.I.
Pumice (wt %)	48	14.9	8.34	8.18	5.70	6.71	1.84	0.62	5.71

Table 1. Chemical composition of pumice determined by X-ray fluorescence

4.2 XRD measurement analysis

Figure 1 displays the X-ray diffraction patterns of the pumice raw material and extracted silica calcined at $800\text{ }^\circ\text{C}$ for two hours. The figure shows that the untreated pumice contains crystalline minerals (Figure 1 (a)), such as clinopyroxene (diopside, augite or basanite types), forsterite and other minerals in small quantities, such as apatite and haematite [1, 22–25]. The strong broad hump, between 15

and 30° (2θ) (Figure 1 (b)) indicates that the silica SiO_2 that was extracted from the pumice powder is amorphous and that no crystalline structure appeared [7, 9, 15]. Furthermore, the absence of peaks indicating possible impurities, such as sodium sulphate and other alkaline earth metals, confirmed the high purity of the derived silica.

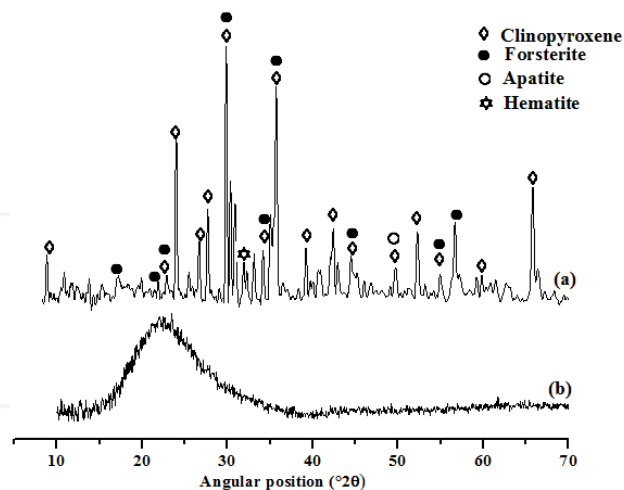


Figure 1. X-ray diffractograms of pumice (a) and amorphous silica (b)

4.3 FTIR spectroscopy analysis

Figure 2 exhibits the FTIR spectra of raw pumice and extracted amorphous silica obtained after calcination at $800\text{ }^\circ\text{C}$ for two hours. In Figure 2 (a), the broadening band that can be observed between 1300 and 820 cm^{-1} is assigned to different mineral oxides present in the pumice material. The narrow band centred at 1039 cm^{-1} may be attributed to the presence of silica. This band confirms the highest percentage of silica in the pumice [1], which is further confirmed by chemical analysis (Table 1). The predominant band at 1101 cm^{-1} and the shoulder at 1193 cm^{-1} in Figure 2 (b) are associated with asymmetric stretching-vibrations of siloxane $\nu_{\text{as}}(\text{Si-O-Si})$. The presence of bands at 470 cm^{-1} and 810 cm^{-1} was due to the presence of symmetric siloxane groups $\nu_{\text{s}}(\text{Si-O-Si})$. The existence of a band at 950 cm^{-1} is associated with Si-OH groups; this band's existence is due to high concentrations of silanol groups with smaller particle sizes [26]. The shoulder appeared at 3750 cm^{-1} , indicating the presence of hydrogen bonds that resulted from interaction between the silanol groups (Si-OH) located at the surface of the nanosilica material [27]. In both materials, the band located at 1640 cm^{-1} is attributed to the O-H bending vibration of the adsorbed molecular water and its corresponding stretching vibration at 3456 cm^{-1} . The presence of water molecules in Figure 2 (b) shows that the chemical formula of amorphous silica is close to that of $\text{SiO}_x \cdot y\text{H}_2\text{O}$. These data gave clear evidence that the extracted amorphous silica from pumice by a base-acid treatment could be a chemically reactive method suitable for catalyst preparations [28].

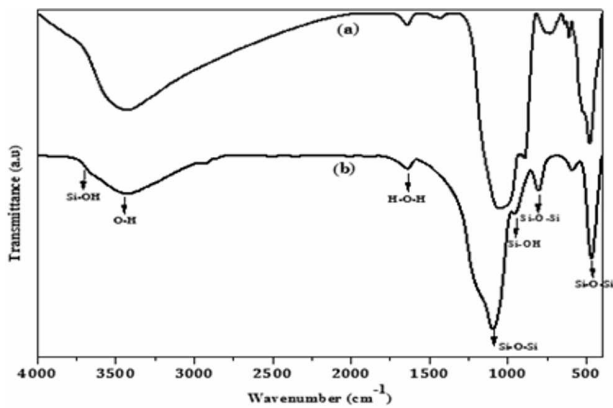


Figure 2. FTIR spectra of pumice (a) and amorphous silica (b)

4.4 TEM-EDS microscopy

The surface morphologies of raw pumice and extracted silica calcined at 800°C for two hours are displayed in Figure 3. Analysis of TEM micrographs illustrates that particles of silica were formed via the acid-base treatment, and that they show a relatively homogenous distribution with spheroidal shapes (Figure 3 (b)). The particle sizes of extracted silica are of a nanometric scale, with diameters in the range of 5–15 nm. The observed diffuse ring pattern is indicative of an amorphous phase consisting of nanosilica. In contrast, the surface morphology of pumice is characterized by the presence of large particles with heterogeneous sizes ranging from 1 μm to quite a few nanometres (Figure 3 (a)). These particles have different geometric patterns.

The EDS data of pumice show the presence of different chemical elements (Figure 4 (a), Table 2), which is in accordance with the XRF and XRD analyses results. The EDS profile of nanosilica particles (Figure 4 (b)) contained (predominantly) the elements of Si and O with a molar ratio of 1.8, which is very close to the stoichiometric ratio 2 of natural silica. This means that the base-acid chemical route has a beneficial effect on the removal of all minerals and impurities from pumice. The EDS, FTIR and XRD results gave clear evidence as to the high purity of amorphous silica extracted from pumice.

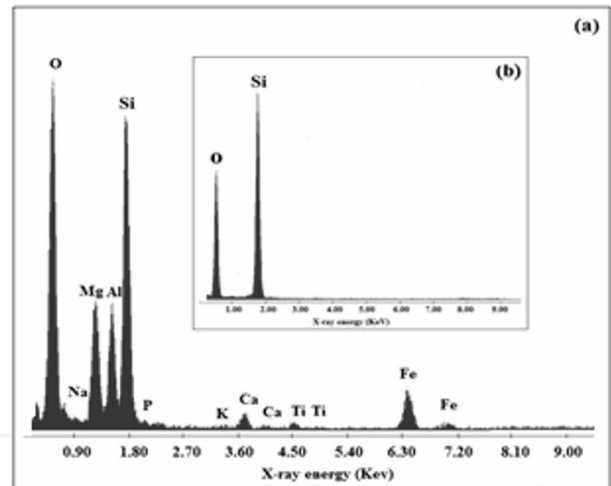
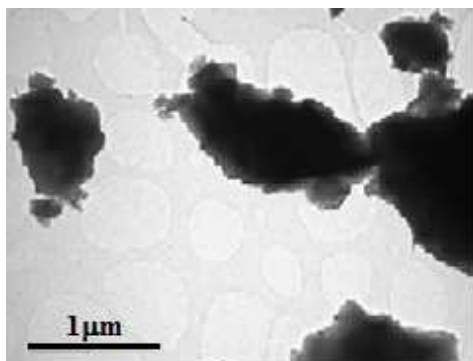


Figure 4. EDS analysis of (a) pumice and (b) extracted nanosilica

Elements	Pumice		Silica	
	Wt %	At %	Wt %	At %
O	24.73	6.4	34.0	46.9
Na	2.7	2.7	-	-
Mg	19.9	19.3	-	-
Al	13.0	11.4	-	-
Si	30.7	25.8	66.0	53.1
P	0.6	0.5	-	-
K	0.0	0.0	-	-
Ca	1.6	0.9	-	-
Ti	0.6	0.3	-	-
Fe	6.2	2.6	-	-
Total	100.0	100.0	100.0	100.0

Table 2. Elemental analysis of pumice and silica determined by EDS

4.5 Textural properties

Both the nitrogen adsorption/desorption measurements at 77 K of the extracted nanosilica powder that was calcined at 800°C for two hours and the pore-size distribution calculated by the Barrett-Joyner-Halenda (BJH) method

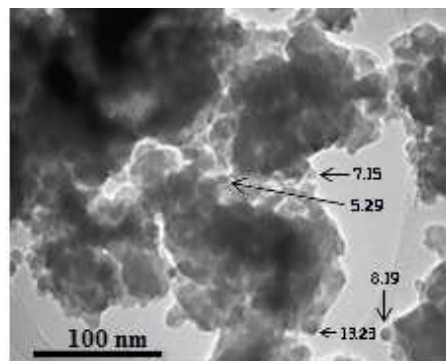


Figure 3. TEM micrographs of (a) pumice and (b) nanosilica particles

using a desorption isotherm are shown in Figure 5. The shape of the isotherms is of a typical IV, with a hysteresis loop representative of mesoporosity, as based on the IUPAC classification [29]. However, this loop does not show any limiting adsorption at a relatively high pressure (P/P^0), which implied that the silica contains slit-shaped pores formed by non-rigid aggregate particles and no pore networks — thus satisfying the main requirements of the BJH method [30, 31]. This result suggests that silica spheres contain an abundance of mesopores. Figure 5 (inset) revealed that silica has a narrow pore-size distribution, with diameters ranging from 2 to 6 nm and an average of 5.5 nm, while the cumulative pore volume of 0.645 exceeds that reported for silica nanoparticles (0.195 cm³/g) derived from rice straw ash [32] and commercial silica (0.220 cm³/g). The Brunauer–Emmett–Teller (BET) surface area of silica powder is 422 m²/g. This particular surface area is much higher than that of commercial silica at 327 m²/g, as well as the 120–288 m²/g surface area reported for the silica nanoparticles derived from rice husk [9, 33].

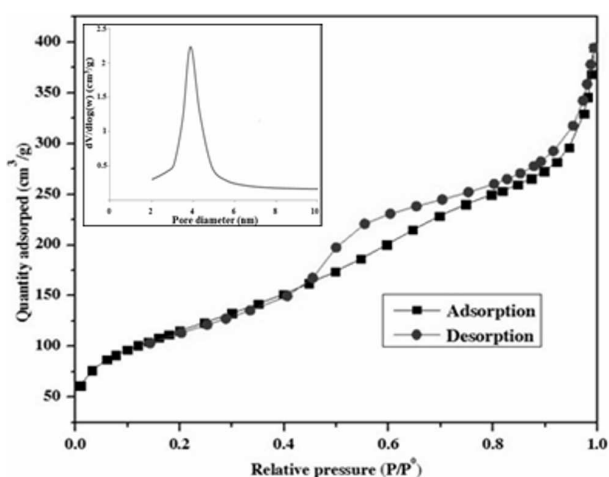


Figure 5. Nitrogen adsorption/desorption isotherms at 77 K of nanosilica particles

4.6 Thermal decomposition characteristics

Figures 6 and 7 illustrate the thermal behaviour of raw pumice and nanosilica powder calcined at 800°C for two hours, at a heating rate of 10°C/min⁻¹ under air atmosphere with a flow rate of 60 ml/min⁻¹. In Figure 6, the observable weight loss of about 6% between 30 and 900°C, with a broad endothermic effect at low temperatures, is due to the removal of moisture as well as that of OH species linked to metal oxides and volatile organic impurities present in small proportions. This result is compatible with XRF analysis (the L.O.I. is 5.71%). A previous thermal analysis study reported that at around 900°C pumice becomes soft and melts completely around 1200°C, which means that pumice can retain its thermal stability until it reaches 900°C [21].

As shown in Figure 7, a DTA thermogram of silica powder showed an intensive endothermic reaction in the range of

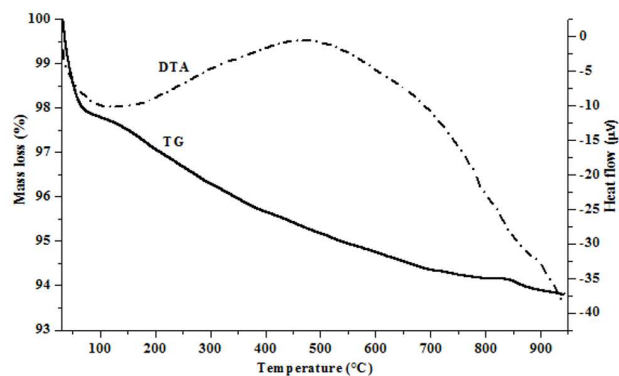


Figure 6. TG-DTA thermograms of raw pumice powder

30–150°C and a shoulder at temperatures beyond 200°C. These peaks are correlated to the loss of physically adsorbed water from the surface (5.2%) and chemically adsorbed water bonded to Si-OH (1.3%) through the hydrogen bond, which corresponds well with the previous results [16]. The total weight loss of pure silica material established from TG analysis is 6.5%.

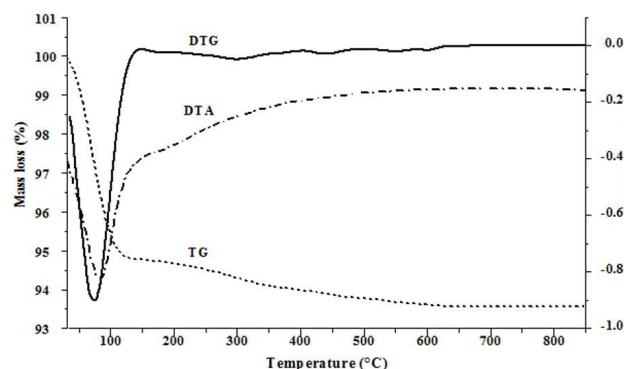


Figure 7. TG-DTG-DTA thermograms of nanosilica powder

Based on results we obtained via TEM-EDS microscopy and TGA analysis, and according to work by I.M. Briman et al., when studying the impact of pore-surface composition on water confined in porous silica [34], the standard chemical formula of synthesized silica can be determined to be $\text{SiO}_{1.78}(\text{OH})_{0.45}$.

5. Conclusion

Highly pure nanosilica powder was obtained via a simple alkaline treatment of cheap local pumice, which contains an appreciable amount of silicates as mineral materials. During the process, the conversion of pumice powder into silica reaches a rate of 94%. This constitutes an important and efficient method for preparing nanosilica with mesoporosity (a pore distribution of 2–6 nm) and a large surface area (422 m²/g), which can be easily produced on a large scale. The FTIR and XRD techniques were confirmed as able to produce amorphous silica with high purity and showed the presence of siloxane and silanol groups. The size and

morphology of silica particles were analysed by TEM-EDS microscopy, which indicated that they are dominated by spheroidal geometry, with diameters of 5–15 nm. The thermal analysis (TG-DTA) of raw pumice was found to be in accordance with XRF analysis, and showed that silica powder contains water molecules bonded physically and chemically to its surface by silanol groups via the hydrogen bond. The amorphous characteristic of the silica, its large-surface area and fine particle size, combined with its low production cost, makes it an ideal candidate for use as a support in catalysis for hydrogen production. The catalytic measurements of hydrogen production via the dry, reforming reaction of methane are in progress.

6. Acknowledgements

This research was supported financially by the University of Mohammed V, Morocco under the Project No. SCH 04/09, and by the Hassan II Academy of Science and Technology, Morocco.

7. References

- [1] Sepehr M N, Zarrabi M, Kazemian H, Amrane A, Yaghmaian K, Ghaffari H R (2013) Removal of hardness agents, calcium and magnesium, by natural and alkaline modified pumice stones in single and binary systems. *Applied Surface Science* 274:295–305. DOI: 10.1016/j.apsusc.2013.03.042.
- [2] Tapan M, Yalçın Z, İçelli O, Kara H, Orak S, Özvan A, Depci T (2014) Effect of physical, chemical and electro-kinetic properties of pumice samples on radiation shielding properties of pumice material. *Annals of Nuclear Energy* 65:290–298. DOI: 10.1016/j.anucene.2013.11.021.
- [3] Al-Naaymi T A, Ali M A (2013) Chemical physical and geotechnical properties comparison between scoria and pumice deposits in Dhamar — Rada volcanic field — SW Yemen. *Australian Journal of Basic and Applied Sciences* 7:116–124.
- [4] Ottanà R, Saija LM, Burriesci N, Giordano N (1982) Hydrothermal synthesis of zeolites from pumice in alkaline and saline environment. *Zeolites* 2:295–298. DOI: 10.1016/S0144-2449(82)80073-0.
- [5] Burriesci N, Arcoraci C, Giordano N, Antonucci P L (1985) Zeolites from pumice and tuff as evaluation of pozzolanic cement constituents. *Zeolites* 5:96–100. DOI: 10.1016/0144-2449(85)90080-6.
- [6] Johnson CD, Worrall F (2007) Zeolitisation of pumice — microporous materials on macroporous support structures derived from natural materials. *Journal of Materials Chemistry* 17:476–484. DOI: 10.1039/B610865B.
- [7] Singh L P, Agarwal S K, Bhattacharyya S K, Sharma U, Ahalawat S (2011) Preparation of silica nanoparticles and its beneficial role in cementitious materials. *Nanomaterials and Nanotechnology* 1:44–51. DOI: 10.5772/50950.
- [8] Essien E R, Olaniyi O A, Adams L A, Shaibu R O (2012) Sol-gel-derived porous silica: economic synthesis and characterization. *Journal of Minerals and Materials Characterization and Engineering* 11:976–981. DOI: 10.4236/jmmce.2012.1110098.
- [9] Lu P, Hsieh Y Lo (2012) Highly pure amorphous silica nano-disks from rice straw. *Powder Technology* 225:149–155. DOI:10.1016/j.powtec.2012.04.002.
- [10] Srivastava K, Shringi N, Devra V, Rani A (2015) A facile method for production of amorphous silica from perlite under microwave irradiation, *International Journal of IT, Engineering and Applied Sciences Research* 4:18–24. DOI: 10.1016/j.apt.2009.03.008.
- [11] Rani A, Sanal S, Jacob T, Jacob G, Desy P K, Manivarnan N K (2014) Silica nano particles synthesized from boiler spent ash: value addition to an industrial waste. *Chemistry and Materials Research* 6:93–99.
- [12] Shen Y, Zhao P, Shao Q (2014) Porous silica and carbon derived materials from rice husk pyrolysis char. *Microporous and Mesoporous Materials* 188:46–76. DOI: 10.1016/j.micromeso.2014.01.005.
- [13] Rani K M, Palanisamy P N, Sivakumar P (2014) Synthesis and characterization of amorphous nanosilica from biomass ash. *International Journal of Advanced Technology in Engineering and Science* 2:71–76.
- [14] Kalapathy U, Proctor A, Shultz J (2002) An improved method for production of silica from rice hull ash. *Bioresource Technology* 85:285–289. DOI: 10.1016/S0960-8524(02)00116-5.
- [15] Kalapathy U, Proctor A, Shultz J (2000) A simple method for production of pure silica from rice hull ash. *Bioresource Technology* 73:257–262. DOI: 10.1016/S0140-6701(01)80487-2.
- [16] Todorova E V, Chernev G E, Djambazov S P (2014) Structure and properties of functionalized porous silica hybrid materials. *Open Journal of Inorganic Non-Metallic Materials* 4:35–43. DOI: 10.4236/ojinm.2014.43006.
- [17] Moreno N, Querol X, Plana F, Andres J M, Janssen M, Nugteren H (2002) Pure zeolite synthesis from silica extracted from coal fly ashes. *Journal of Chemical Technology and Biotechnology* 77:274–279. DOI: 10.1002/jctb.578.
- [18] Thuadaj N, Nuntiya A (2008) Preparation of nanosilica powder from rice husk ash by precipitation method. *Chiang Mai Journal of Science* 35:206–211.
- [19] Patil R, Dongre R, Meshram J (2014) Preparation of silica powder from rice husk. *Journal of Applied Chemistry*. 27:26–29.

- [20] Adam F, Chew T S, Andas J (2011) A simple template-free sol-gel synthesis of spherical nanosilica from agricultural biomass. *Journal of Sol-Gel Science and Technology* 59:580–583. DOI: 10.1007/s10971-011-2531-7.
- [21] Ersoy B, Sariisik A, Dikmen S, Sariisik G (2010) Characterization of acidic pumice and determination of its electrokinetic properties in water. *Powder Technology* 197:129–135. DOI: 10.1016/j.powtec.2009.09.005.
- [22] Nasser S, Heidari M (2012) Evaluation and comparison of aluminum coated-pumice and zeolite in arsenic removal from water resources. *Iranian Journal of Environmental Health Science and Engineering* 9:256–268. DOI: 10.1186/1735-2746-9-38.
- [23] Mahvi A H, Heibati B, Mesdaghinia A, Yari A R (2012) Fluoride adsorption by pumice from aqueous solutions. *E-Journal of Chemistry* 9:1843–1853. DOI: 10.1155/2012/581459.
- [24] Tapan M (2014) Use of pumice and scoria aggregates for controlling alkali silica reaction. *Physicochemical Problems of Minerals Processing* 50:467–475.
- [25] Cekova B, Pavlovski B, Spasev D, Reka A (2013) Structural examinations of natural raw materials pumice and trepel from republic of Macedonia: Balkan Mineral Processing Congress, Bulgaria p. 73–75.
- [26] Rahman I A, Vejayakumaran P, Sipaut C S, Ismail J, Chee C K (2009) Size-dependent physicochemical and optical properties of silica nanoparticles. *Materials Chemistry and Physics* 114:328–332. DOI: 10.1016/j.matchemphys.2008.09.068.
- [27] Yang J, Wang E (2006) Reaction of water on silica surfaces. *Current Opinion in Solid State and Materials Science* 10:33–39. DOI: 10.1016/j.cossms.2006.02.001.
- [28] Lai C Y (2013) Mesoporous nanomaterials applications in catalysis. *Journal of Thermodynamics & Catalysis* 5:1–3. DOI: 10.4172/2157-7544.1000e124.
- [29] Sing K S W, Everett D H, Haul R A W, Moscou L, Pierotti R A, Rouquerol J, Siemieniewska T (1985) Reporting physisorption data for gas/solid systems with special reference to the determination of surface area and porosity. *Pure and Applied Chemistry* 57:603–619. DOI: 10.1351/pac198557040603.
- [30] Horikawa T, Do D D, Nicholson D (2011) Capillary condensation of adsorbates in porous materials. *Advances in Colloid and Interface Science* 169:40–58. DOI: 10.1016/j.cis.2011.08.003.
- [31] Cendrowski K, Chen X, Zielinska B, Kalenczuk R J, Rümmele M H, Büchner B, Klingeler R, Borowiak-Palen E (2011) Synthesis, characterization, and photocatalytic properties of core/shell mesoporous silica nanospheres supporting nanocrystalline titania. *Journal of Nanoparticle Research* 13:5899–5908. DOI: 10.1007/s11051-011-0307-1.
- [32] Hessian MM, Rashad MM, Zaky RR, Abdel-Aal EA, El-Barawy KA (2009) Controlling the synthesis conditions for silica nanosphere from semi-burned rice straw. *Materials Science and Engineering B: Solid-State Materials for Advanced Technology* 162:14–21. DOI: 10.1016/j.mseb.2009.01.029.
- [33] Zhang H, Zhao X, Ding X, Lei H, Chen X, An D, Li Y, Wang Z (2010) A study on the consecutive preparation of d-xylose and pure superfine silica from rice husk. *Bioresource Technology* 101:1263–1267. DOI: 10.1016/j.biortech.2009.09.045.
- [34] Briman I M, Rébiscoul D, Diat O, Zanotti J M, Jollivet P, Barboux P, Gin S (2012) Impact of pore size and pore surface composition on the dynamics of confined water in highly ordered porous silica. *Journal of Physical Chemistry C* 116:7021–7028. DOI: 10.1021/jp3001898.